Microgravity Sci. Technol. (2016) 28:575–585
DOI 10.1007/s12217-016-9513-x

ORIGINAL ARTICLE

Development of Concentration-Dependent Diffusion Instability in Reactive Miscible Fluids Under Influence of Constant or Variable Inertia

Dmitry A. Bratsun[1] · Olga S. Stepkina[2] · Konstantin G. Kostarev[3] · Alexey I. Mizev[3] · Elena A. Mosheva[3]

Received: 31 January 2016 / Accepted: 25 July 2016 / Published online: 6 August 2016

Abstract In this work, we focus on the processes which accompany a frontal neutralization reaction occurring between two miscible fluids filling a vertical Hele-Shaw cell. We have found that chemically-induced changes of reagent concentrations coupled with concentration- dependent diffusion (CDD) can produce spatially localized low density areas which are sensitive to the external inertial field. In the case of static gravity we have demonstrated both experimentally and theoretically that it can give rise to the development of perfectly periodic convective structure. This scenario is strikingly different from the irregular density fingering, which is typically observed in the miscible systems. When the system is under the influence of the periodic low-frequency vibrations perpendicular to the reaction front, we found numerically the excitation of a mixed-mode instability combining the double-diffusion instabilities and the Rayleigh-Taylor mechanism of the convection within the low density areas.

This article belongs to the Topical Collection: Advances in Gravity-related Phenomena in Biological, Chemical and Physical Systems
Guest Editors: Valentina Shevtsova, Ruth Hemmersbach

✉ Dmitry A. Bratsun
dmitribratsun@rambler.ru

[1] Department of Applied Physics, Perm National Research Polytechnical University, 614990, Perm, Russia

[2] Theoretical Physics Department, Perm State Humanitarian Pedagogical University, 614990, Perm, Russia

[3] Institute of Continuous Media Mechanics, 614013, Perm, Russia

Keywords Chemo-hydrodynamics · Miscible fluids · Finite-frequency vibrations · Neutralization reaction

Introduction

In last decades the interaction between reaction- diffusion phenomena and pure hydrodynamic instabilities has attracted increasing interests because the chemically induced changes of fluid properties such as concentration, density, viscosity, surface tension or adsorption may result in the instabilities, which exhibit a large variety of convective patterns.

The simple, irreversible chemical scheme such as a neutralization reaction $A + B \rightarrow S$ occurring in binary liquid-liquid miscible systems was studied in Almarcha et al. (2010), Almarcha et al. (2011), Carballido-Landeira et al. (2013) and Trevelyan et al. (2015). The irregular plumes and fingers commonly observed here when the heavier fluid A overlies the lighter fluid B. This stratification is unstable under gravity via the Rayleigh-Taylor (RT) mechanism (Almarcha et al. 2010; Fernandez et al. 2002). It should be noted that, in nonreactive miscible systems, buoyancy-driven instabilities lead to convective motions which develop similarly above and below the initial contact since the underlying density gradient is symmetric (Fernandez et al. 2002). By contrast, the convection triggered by the reaction develops asymmetric patterns with respect to the initial position of the interface (Almarcha et al. 2010). Another important engine breaking the equilibrium in the miscible systems was found to be the difference between the diffusion rates of species resulting in double diffusive instability (DD) or diffusive-layer convection (DLC) (Almarcha et al. 2011; Carballido-Landeira et al. 2013; Trevelyan et al. 2015). It may occur when the upper fluid is lighter, but

B diffuses faster than *A* (DD fingering), or *A* diffuses faster than *B* (DLC). And again, in nonreactive miscible fluids, the double-diffusion convective motions are symmetric (Turner 1974), but the reaction produces asymmetric patterns (Almarcha et al. 2010; Lemaigre et al. 2013).

Recently, we have reported a new type of instability, *the concentration-dependent diffusion* (CDD) instability (Bratsun et al. 2015; Aitova et al. 2015). The CDD convection belongs to the family of the double-diffusion phenomena, and it arises when the diffusion coefficients of species depend on their concentrations. In contrast with previous works, we have shown that chemically-induced changes of reagent concentrations coupled with concentration-dependent diffusion can produce spatially localized zone with unstable density stratification that under gravity gives rise to the development of perfectly regular cell-like convective pattern even in the miscible system. The effect was found primarily for the pair HNO_3/NaOH, but then it was demonstrated also for other systems (for example, HNO_3/KOH, HCl/NaOH). The described effect has given an example of yet another powerful mechanism which allows the reaction-diffusion processes to govern the fluid flow under gravity condition.

Although the concentration dependence of the diffusion coefficients of species has been rarely considered in the fluid mechanics, some analogy can be drawn, for example, with viscous fingering in miscible displacement flows in porous media (Hickernell and Yortsos 1986; Manickam and Homsy 1993, 1994, 1995; Loggia et al. 1995). Both the concentration-dependent viscosity and the heterogeneity in the permeability of the porous medium can produce the simple nonmonotonicity in the mobility profiles somewhat similar to those in the reactive case. The first paper (Hickernell and Yortsos 1986) devoted to the issue has examined the linear stability of miscible displacement processes in simplified formulation (without diffusion and dispersion), but including the influence of gravity. Then the effect of the nonmonotonic viscosity profile on the miscible displacements has been considered in the series of works (Manickam and Homsy 1993, 1994, 1995) where both linear and nonlinear phenomena have been studied. Finally, some predictions of theoretical works have been verified experimentally in Loggia et al. (1995).

The possibility of appearance of a parametrically excited convective instability has first been emphasized in Gershuni and Zukhovitskii (1963) where a plane horizontal layer of a fluid heated from below under a periodic modulation of the gravity force was considered. This result was experimentally confirmed later in Putin et al. (1992) and Rogers et al. (2000). As for inhomogeneous fluids, the instability of a small transient diffusive layer between two miscible liquids under finite-frequency vibrations was found experimentally and numerically in Gaponenko et al. (2015). The similar effect are observed in the dusty fluids. There are a number of papers (see, for example, Bratsun and Teplov 2000; Bratsun 2009) showing that a fine heavy admixture to nonreactive fluids may exert, under certain conditions, a significant effect on flow stability and structure.

Unlike the nonreactive case, the miscible reacting fluids placed in a variable inertial field seems to be more complicated system, as the concentrations of reactants may vary locally in real-time due to the ongoing volume reaction. For example, one should mention works concerning the development of frontal polymerization under different vibrations (Allali et al. 2002). It was shown that vibrations can stabilize the polymerization front. In recent years, more and more interest of researchers is attracted to the chemo-hydrodynamic systems in the variable inertial field (Eckert et al. 2012; von Kameke et al. 2010, 2013). The dynamics of neutralization reaction fronts under modulated gravitational acceleration by means of a combination of parabolic flight experiments and numerical simulations was studied in Eckert et al. (2012). It was shown that the front position also undergoes periodic modulation with an accelerated front propagation under hyper-gravity together with a slowing down under low gravity because of corresponding an amplification and a decay, respectively, of the buoyancy-driven vortex. In von Kameke et al. (2010, 2013) the authors have considered an alternate way of inertial action on the system, namely, high-frequency vertical vibrations applied to the reacting fluid layer with free surface, in which case the effect of hydrodynamics is quite evident. In this situation, the hydrodynamic effect induced by the Faraday ripple occurs on the upper free boundary, giving rise to the surface turbulence, so that the reaction-diffusion processes pass through quite another pattern of dynamic evolution.

Generally, the frontal reaction can generate inhomogeneous densities, which in the constant field can lead to the onset of different types of instability. Obviously, such reacting systems are subject to the action of external variables and inhomogeneous inertial fields. However, up to now there has been no systematic work done to investigate this influence neither for finite-frequency nor high-frequency vibrations.

In this work we study a Hele-Shaw flow, i.e. the flow of a fluid between two plates which are close to each other. A review of the early works devoted to the Hele-Shaw flows is given in Homsy (1987). Since the governing equations of the fluid in the Hele-Shaw cell with an infinitesimally small gap are similar to those for the porous medium, one can use the Hele-Shaw cell to accurately predict what happens in the latter case. With some reservations, this approach also works in the opposite direction. This is why one often uses the law of Darcy to study the Hele-Shaw flows (Carballido-Landeira et al. 2013; Trevelyan et al. 2015; Fernandez et al. 2002; Homsy 1987). However, if the gap

between the plates is small, but finite, the averaging across the Hele-Shaw should be made by taking into account the inertial terms (Ruyer-Quil 2001; Martin et al. 2002a). A more systematic discussion of the so-called Brinkman correction for the Hele-Shaw flows is given in Zeng et al. (2003). The application of such approach to the buoyancy-driven instability of an autocatalytic reaction front was first considered in Martin et al. (2002b). An important result was obtained in Martin et al. (2011), where the authors demonstrated analytically and experimentally that the Hele-Shaw averaging leads to a rather good approximation, when an appropriate Brinkman correction is used. The importance of this approach was also found in Bratsun and De Wit (2004) for the two-layer Hele-Shaw system with an exothermic chemical reaction. Obviously, in the case of an alternating inertial field the effect of the Brinkman term becomes particularly important.

The goal of the present work is to study the effect of low-frequency vertical vibrations on the concentration-dependent diffusion convection that arises during a frontal neutralization reaction occurring between two miscible fluids filling a vertical Hele-Shaw cell.

Theoretical Model

Let two miscible liquids fill a Hele-Shaw cell. A Hele-Shaw cell is a closed parallelepiped cavity significantly compressed in one of the horizontal directions (Fig. 1). The upper and lower layer are aqueous solutions of acid A and base B respectively. Right after the process starts, the acid and base diffuse into each other and are neutralized according to $A + B \rightarrow S$ with the formation of salt S with the rate K. The neutralization reaction is exothermic, but, for simplicity, here we consider the system shown in Fig. 1 as isothermal. The system geometry is given by three-dimensional domain with x- and y-axes directed horizontally and z-axis anti-directed to gravity. The cell boundaries are defined to be $0 \le x \le H$, $-d \le y \le d$, $-L \le z \le L$. Then $z = 0$ determines the initial contact plane between the reacting species.

We start with the set of reaction-diffusion-convection equations applicable to a viscous fluid of varying density depending on concentrations:

$$\nabla \cdot \mathbf{U} = 0, \tag{1}$$

$$\frac{\partial \mathbf{U}}{\partial t} + \mathbf{U} \cdot \nabla \mathbf{U} = -\frac{1}{\rho_0}\nabla P + \nu \triangle \mathbf{U} - (g\mathbf{z} + \mathbf{n}b\omega^2 cos(\omega t)) \times (\beta_a A + \beta_b B + \beta_s S), \tag{2}$$

$$\frac{\partial A}{\partial t} + \mathbf{U} \cdot \nabla A = \nabla D_a(A) \nabla A - KAB, \tag{3}$$

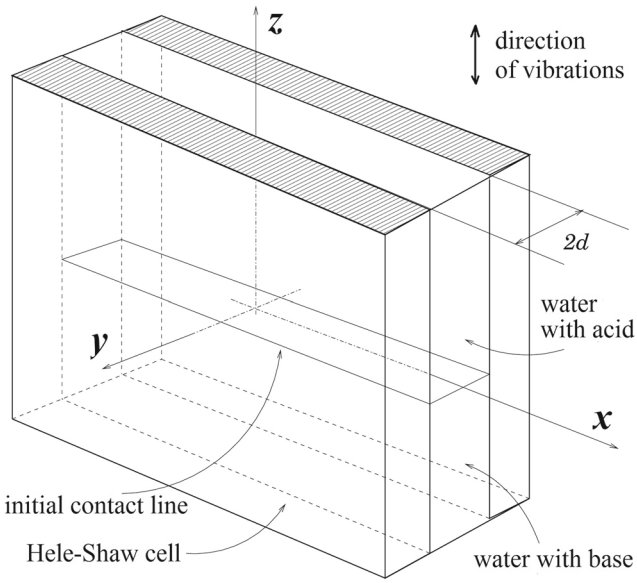

Fig. 1 Geometrical configuration of the two-layer miscible system and coordinate axes

$$\frac{\partial B}{\partial t} + \mathbf{U} \cdot \nabla B = \nabla D_b(B) \nabla B - KAB, \tag{4}$$

$$\frac{\partial S}{\partial t} + \mathbf{U} \cdot \nabla S = \nabla D_s(S) \nabla S + KAB, \tag{5}$$

where $\mathbf{U}(U_x, U_y, U_z)$ is the velocity, P is the pressure and A, B, S are the concentrations of species. $\mathbf{z}$ is the unit vector along the z-axis. The density of fluid and kinematic viscosity are, respectively, equal to ρ_0, ν. The amplitude and frequency of vibrations are denoted as b and ω respectively. In this work we suppose that the vibrations are co-directed to gravity vector: $\mathbf{n} = \mathbf{z}$. The diffusion terms in Eqs. 3–5 have been written in the most general form (Bratsun et al. 2015; Crank 1975).

We assume further that the gap-width $2d$ between the plates is small enough (see Fig. 1) so that the fluid flow may be considered as quasi two-dimensional, i.e. a Hele-Shaw approximation is applicable (Ruyer-Quil 2001; Martin et al. 2002a; Bratsun and De Wit 2011). Taking into account the standard boundary conditions for velocity and concentration on solid plates one can assume the following approximations:

$$U_x(x, y, z) = \frac{3}{2}\left(1 - \frac{y^2}{d^2}\right) v_x(x, z), \tag{6}$$

$$U_y(x, y, z) = 0, \tag{7}$$

$$U_z(x, y, z) = \frac{3}{2}\left(1 - \frac{y^2}{d^2}\right) v_z(x, z), \tag{8}$$

$$A = A(x, z), \quad B = B(x, z), \quad S = S(x, z), \tag{9}$$

where $\mathbf{v}(v_x, v_z)$ is two-component velocity field. Then the evolution equations in a Hele-Shaw approximation are obtained by inserting (6)–(9) into the three- dimensional Navier-Stokes equations (1)–(2) coupled to heat and reaction-diffusion equations (3)–(5), and averaging with respect to the y-space direction perpendicular to the solid plates:

$$< ... >= \frac{1}{2d}\int_{-d}^{d} ...dy. \tag{10}$$

We choose the following units of measurement: length - $2d$, time - $4d^2/D_{a0}$, velocity - $D_{a0}/2d$, concentration - A_0, pressure - $\rho_0 \nu D_{a0}/4d^2$. Here D_{a0} and A_0 define constant acid diffusivity and initial acid concentration respectively. By averaging the equations (1)–(5) with respect to Eq. 10 we shall get the convection-reaction-diffusion equations in a Hele-Shaw approximation:

$$\Phi = -\triangle\Psi, \tag{11}$$

$$\frac{1}{Sc}\left(\frac{\partial\Phi}{\partial t} + \frac{6}{5}\frac{\partial(\Psi,\Phi)}{\partial(z,x)}\right) = \triangle\Phi - 12\Phi$$
$$-R_a\frac{\partial A}{\partial x} - R_b\frac{\partial B}{\partial x} - R_s\frac{\partial S}{\partial x}$$
$$-\left(G_a\frac{\partial A}{\partial x} + G_b\frac{\partial B}{\partial x} + G_s\frac{\partial S}{\partial x}\right)cos(\Omega t), \tag{12}$$

$$\frac{\partial A}{\partial t} + \frac{\partial(\Psi,A)}{\partial(z,x)} = \nabla D_a(A)\nabla A - \alpha AB, \tag{13}$$

$$\frac{\partial B}{\partial t} + \frac{\partial(\Psi,A)}{\partial(z,x)} = \nabla D_b(B)\nabla B - \alpha AB, \tag{14}$$

$$\frac{\partial S}{\partial t} + \frac{\partial(\Psi,S)}{\partial(z,x)} = \nabla D_s(S)\nabla S + \alpha AB. \tag{15}$$

Here we use a two-field formulation for movement equation introducing the stream function Ψ:

$$v_x = \frac{\partial\Psi}{\partial z}, \qquad v_z = -\frac{\partial\Psi}{\partial x},$$

and the vorticity Φ defined by Eq. 11. The advection terms in Eqs. 12–15 have been written in the compact form of the Jacobian determinant:

$$\frac{\partial(\zeta,\xi)}{\partial(z,x)} = \frac{\partial\zeta}{\partial z}\frac{\partial\xi}{\partial x} - \frac{\partial\zeta}{\partial x}\frac{\partial\xi}{\partial z}.$$

The Eq. 12 differ from a standard Navier-Stokes equation by one more additional term linear in the vorticity. This term appearing within the Hele-Shaw approximation may be interpreted as the average friction force due to the presence of the plates and are analogous to the linear velocity term in Darcy's law valid for fluid flow in porous media.

The boundary conditions for Eqs. 11–15 are

$$x = 0, H: \Psi = 0, \frac{\partial\Psi}{\partial x} = 0, \frac{\partial A}{\partial x} = 0, \frac{\partial B}{\partial x} = 0, \frac{\partial S}{\partial x} = 0.$$

$$z = \pm L: \Psi = 0, \frac{\partial\Psi}{\partial z} = 0, \frac{\partial A}{\partial z} = 0, \frac{\partial B}{\partial z} = 0, \frac{\partial S}{\partial z} = 0, \tag{16}$$

Finally, the initial conditions are defined as

$$z < 0: \quad \Psi = 0, \quad \frac{\partial\Psi}{\partial z} = 0, \quad A = 0, \quad B = 1,$$

$$z > 0: \quad \Psi = 0, \quad \frac{\partial\Psi}{\partial z} = 0, \quad A = 1, \quad B = 0. \tag{17}$$

We have found in Bratsun et al. (2015) and Aitova et al. (2015) that a concentration- dependence of diffusion plays an important role in the pattern formation. It demands that the diffusion coefficients in Eqs. 13–15 of the mathematical model should be assumed not to be constant, but depend on their own concentrations: $D_a(A)$, $D_b(B)$ and $D_s(S)$. Of course, for each pair of reagents, these dependencies are unique and different from data for other pairs. To be specific, we focus here on a pair of reagents HNO_3/NaOH for which we have brought together in Bratsun et al. (2015) all the known experimental data and have constructed a linear approximation within the experimentally interesting range of concentration from 0.1 to 3 mol/l:

$$D_a(A) \approx 0.881 + 0.158A, \tag{18}$$

$$D_b(B) \approx 0.594 - 0.087B, \tag{19}$$

$$D_s(S) \approx 0.478 - 0.284S, \tag{20}$$

where the formulas are already given in the dimensionless form.

The full list of dimensionless parameters appeared in the system of Eqs. 11–20 is given in the Table 1. Their values for the pair HNO_3 / NaOH have been estimated as follows: $Sc \approx 10^3, \alpha \approx 10^3, R_a = 1.5 \times 10^3, R_b = 1.8 \times 10^3, R_s = 2.4 \times 10^3$. The solutal Gershuni numbers are proportional to the Rayleigh numbers: $G_i = \mu R_i$, where $i = \{a, b, s\}$. Here $\mu = b\omega^2/g$ stands for the dimensionless amplitude of vibrations.

Table 1 List of dimensionless parameters

Definition	Name of the parameter
$Sc = \nu/D_{a0}$	Schmidt number
$R_a = g\beta_A A_0(2d)^3/D_{a0}\nu$	Rayleigh number for acid
$R_b = g\beta_B A_0(2d)^3/D_{a0}\nu$	Rayleigh number for base
$R_s = g\beta_S A_0(2d)^3/D_{a0}\nu$	Rayleigh number for salt
$G_a = b\omega^2\beta_A A_0(2d)^3/D_{a0}\nu$	Gershuni number for acid
$G_b = b\omega^2\beta_B A_0(2d)^3/D_{a0}\nu$	Gershuni number for base
$G_s = b\omega^2\beta_S A_0(2d)^3/D_{a0}\nu$	Gershuni number for salt
$\Omega = \omega(2d)^2/D_{a0}$	frequency of vibrations
$\alpha = KA_0(2d)^2/D_{a0}$	Damköhler number
$\mu = b\omega^2/g$	amplitude of vibrations

In order to describe the effect in term of the buoyancy it is convenient to introduce the total dimensionless density:

$$\rho(t,x,z) = R_a A(t,x,z) + R_b B(t,x,z) + R_s S(t,x,z) \quad (21)$$

and the variable inertial field:

$$I(t) = 1 + \mu cos(\Omega t), \quad (22)$$

with $I(t)\rho(t,x,z)$ representing the term of a volume vibration force in Eq. 2.

In the particular case of no static component of the gravity $g = 0$, the Eqs. 21 and 22 should be rewritten in the form, respectively:

$$\rho^0(x,z) = G_a A(x,z) + G_b B(x,z) + G_s S(x,z), \quad (23)$$

$$I^0(t) = cos(\Omega t). \quad (24)$$

Base State

The system of Eqs. 11–20 allows for an important class of nonsteady solutions, which describe dynamics of the reaction-diffusion processes with liquid to remain in the state of mechanical equilibrium. Let us term this state of the system as the base state. Then we consider the concentration fields depending solely from the vertical axis and time: $A^0(t,z)$, $B^0(t,z)$, $S^0(t,z)$. Then we get:

$$\frac{\partial A^0}{\partial t} = D_a(A^0)\frac{\partial^2 A^0}{\partial z^2} + \frac{\partial D_a(A^0)}{\partial z}\frac{\partial A^0}{\partial z} - \alpha A^0 B^0, \quad (25)$$

$$\frac{\partial B^0}{\partial t} = D_b(B^0)\frac{\partial^2 B^0}{\partial z^2} + \frac{\partial D_b(B^0)}{\partial z}\frac{\partial B^0}{\partial z} - \alpha A^0 B^0, \quad (26)$$

$$\frac{\partial S^0}{\partial t} = D_s(S^0)\frac{\partial^2 S^0}{\partial z^2} + \frac{\partial D_s(S^0)}{\partial z}\frac{\partial S^0}{\partial z} + \alpha A^0 B^0. \quad (27)$$

The problem (18)–(20), (25)–(27) with boundary and initial conditions (16), (17) is a non-linear reaction-diffusion problem and can be solved only numerically. Figure 2 shows the base state profiles of the total density $\rho(z)$ for three consecutive time moments $t = 0, 2, 10$. One can see that just after the evolution starts, the density profile has two minima (above and below the reaction front initially located at $z = 0$). Under the constant gravity condition the minimum at $z > 0$ looks to be the typical condition for the asymmetric diffusive layer convection (DLC) to occur (Almarcha et al. 2010). We work in the parameter ranges where the DLC instability is believed to be primary (Trevelyan et al. 2015). It can be described as the instability which starts when a given solution overlies a denser solution, but the solute on top diffuses faster than the one on the bottom.

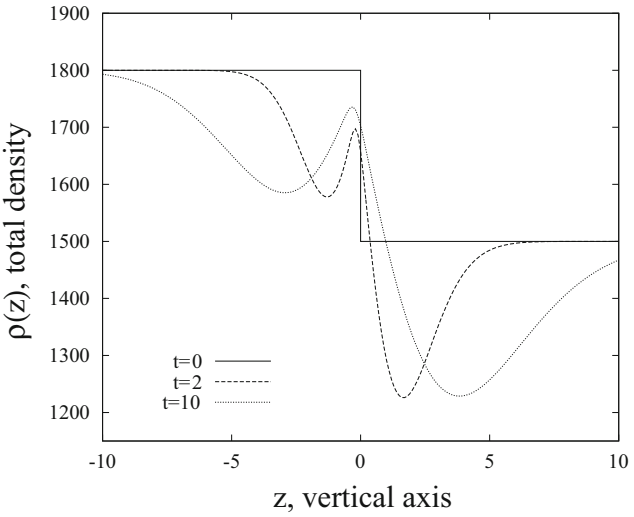

Fig. 2 Instantaneous base state profiles of the total density $\rho(z)$ at times $t = 0, 2, 10$

Since $R_a = 1.5 \times 10^3$, $R_b = 1.8 \times 10^3$ and the diffusion coefficients of species is defined by Eqs. 18–20, this is exactly our case. In the course of evolution, the classic DLC instability inevitably triggers irregular fingering above and below the initial contact line.

However, we have shown in Bratsun et al. (2015) for the reactive case that the minimum at $z < 0$ enclosed within the regions with a stable stratification (with respect to static gravity) occurs exclusively due to the concentration-dependence of diffusion (CDD). This is why we have named it as the CDD instability. It may occur only in the reactive case when an emerging component starts to accumulate near the reaction front. If its molecules quickly leave the reaction zone, then it has no significant influence on the instability scenario. But if the diffusion coefficient of the reaction product decreases with growth of its concentration, as it happens in Eq. 20, it can progressively make a "density pocket", i.e. the local minimum in the density profile (Fig. 2). Thus, the DLC instability can trigger the fingering process only above the initial contact line.

When the inertial field becomes variable, the complex density stratification produced due to the reaction creates opportunities for the development of various types of disturbances. Assume for the simplicity that the static component is absent $g = 0$, the inertial field is perpendicular to the initial contact line of reagents, and the inertia itself varies periodically according to Eq. 24. Figure 3 demonstrates the areas of the unstably stratified density for two successive moments of time separated by a half-period of vibrations. When the inertia force is directed to the left (Fig. 3, top), one may expect that the DLC instability occurs since the acid solution is placed above the a denser base solution with the fastest diffusing solute being in the upper layer.

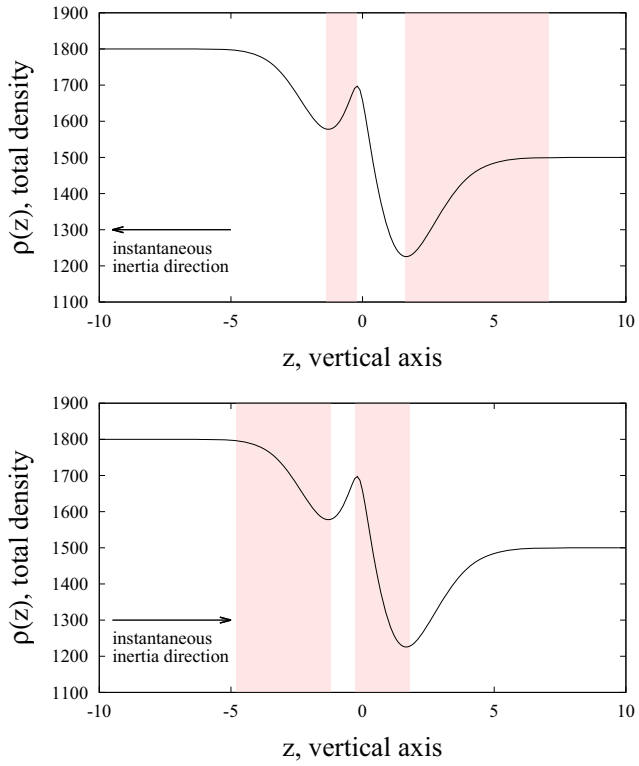

Fig. 3 The areas of the unstable stratification of the total density $\rho(z)$ for two successive moments of time separated by a half-period of vibrations. The instantaneous direction of the inertial field is indicated in the figures

Another area located below the initial contact line corresponds to the CDD instability discussed above. When the inertia force changes its sign (Fig. 3, bottom), one has the situation of a "heavy on top of light", which is naturally unstable with regard to the Rayleigh-Taylor instability. In this case, one can expect a much smaller role of the effect of double diffusion phenomena.

Results of Numerical Simulation

The problem (11)–(20) has been solved numerically by a finite-difference method. A detailed description of the method is given in Bratsun (2014). An explicit scheme has been used, and in order to ensure the stability of the method, the time step was calculated by the formula

$$\triangle t = \frac{\triangle x^2}{2(2 + max(|\Psi|, |\Phi|))}. \tag{28}$$

Here $\triangle x$ is a mesh size for the corresponding coordinate. The Poisson equations are solved by the iterative Liebmann successive over-relaxation method at each time step: the accuracy of the solution is fixed to 10^{-4}. The approximation for a vorticity providing the second order of accuracy was used on the horizontal solid boundaries:

$$\Phi(x, \pm L) = \pm \frac{\Psi(x, \pm L \mp 2\triangle z) - 8\Psi(x, \pm L \mp \triangle z)}{2\triangle z}. \tag{29}$$

Two kinds of boundary conditions have been applied at $x = 0, H$. The first one is the condition of periodicity for all fields, and the second one includes the no-flux condition for species and no-slip condition for the stream function and vorticity. Numerical simulations have showed no significant difference between these two cases. We have performed the calculations at uniform rectangular mesh. The typical resolution was 5×5 nodes for a square of unit side. For example, for the area $H = 40$, $L = 30$ we used the mesh 200 by 300. As the initial condition we applied a noisy distribution of the stream function with amplitude less than 10^{-3}.

Static Inertial Field

Figure 4 presents the time evolution of the stream function maximum separately calculated for the part of the domain above ($z > 0$) and below ($z < 0$) the initial contact line. Since we consider the case of miscible liquids, at first glance, such a separation does not look very reasonable. But two different chemo-convective instabilities were found to arise independently in the upper and lower part of the domain. Thus, each maximal stream function characterizes the development of its own instability. The evolution of the total density $\rho(t, x, z)$ defined by Eq. 21 is illustrated by the frames for three consecutive moments of time in Fig. 5.

The dynamics of the system has been developing almost independently in the upper and lower parts of it, and can be divided in several stages. First, a pure reaction-diffusion process takes place up to $t \approx 3$ (Fig. 5, $t = 3$). Then, the convection arises, first in the lower layer where the cellular chemoconvection with a perfectly periodic structure induced by the concentration-dependent diffusion mechanism has been observed (Fig. 5, $t = 4$). The instability

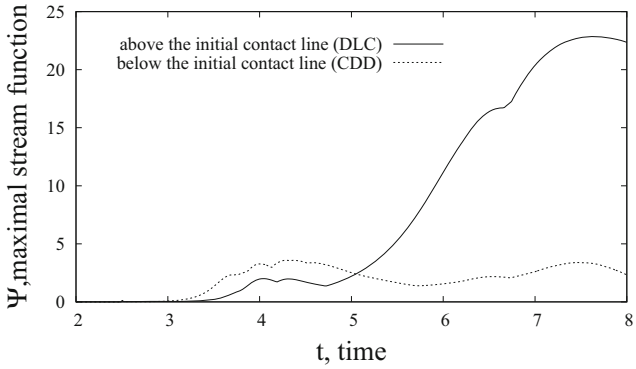

Fig. 4 Time evolution of the maximal stream function of the system under the static gravity field. The values calculated for the *lower* and *upper* layer are indicated by the *dashed* and *solid line*, respectively

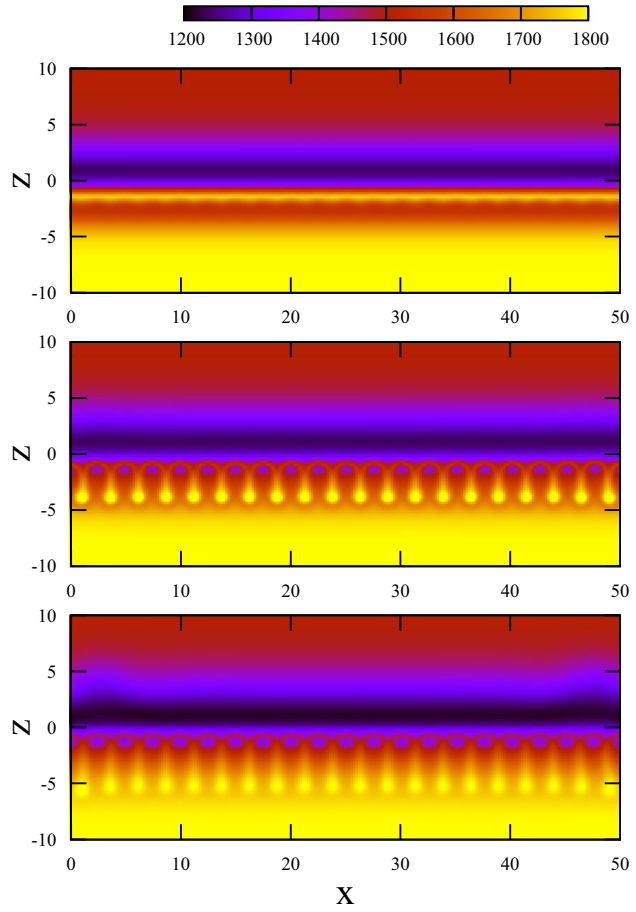

Fig. 5 Time evolution of the total density $\rho(t, x, z)$. The *frames* from *up* to *down* pertain to times $t = 3, 4, 5$, respectively. The integration domain is $0 < x < 70$, $-30 < z < 30$, but only part of the full domain is shown: $0 < x < 50$, $-10 < z < 10$. The *line* $z = 0$ corresponds to the initial contact line between layers

occurs inside the "density pocket", i.e. the local minimum in the density profile (Fig. 2). The resulting convection in the lower layer at the very beginning looks like the fingering process manifesting itself in the acceleration of the movement of the finger tips away from the contact line (Fig. 5, $t = 5$). The main driving force behind this movement is the heavy droplets of salt that fall into the zone of the low density. But since the density pocket is enclosed within the regions with a stable stratification, the fingering process is weakening (see Fig. 4, dashed line), and the convection can develop further only at the expense of the overall growth of the pocket width due to diffusion (Fig. 2). Thus, the mass transfer in the lower layer generally develops under the control of the diffusion processes. Another consequence of the existence of a local minimum density is a leveling effect on the envelope of the chemoconvective structures. This is why the structure shown in Fig. 5 appears uncommonly for the fingering process. We have found in Bratsun (2014) that the salt fingers can be leveled via the Rayleigh-Bénard mechanism, i.e. due to heat release of the exothermic reaction. Now it is clear that there are other mechanisms of the leveling. The occurrence of a local minimum density due to concentration-dependence of the diffusion coefficients of species is one of these mechanisms.

In the upper domain the diffusive layer convection trigger the vigorous fingering process above the initial contact line, which manifest itself in a sharp rise of the stream function maximum at $t > 5$ (see Fig. 4, solid line). Thus, the mass transfer in the upper layer develops under the control of the convective processes. Since the DLC instability many times was described in the literature (see, for example, Trevelyn et al. 2015; Turner 1974; Lemaigre et al. 2013), we do not focus on it here in detail.

We only mention here that the wavelengths of the CDD and DLC instabilities are substantially different, because of the different characteristic widths of two density minima (Fig. 3). The solution of a nonsteady linear stability problem obtained in Bratsun et al. (2015) has shown that at the very beginning the DLC instability wavelength is about six times more than the wavelength of the CDD convection. Over time, the wavelengths of the developed perturbations gradually converge in magnitude.

Variable Inertial Field

Figure 6 presents the time evolution of the stream function maximum under the influence of a periodically varied inertial field I (24). The amplitude of vibrations is $\mu = 4$ and the period is $\tau = 0.1$. The dynamics in the upper ($z > 0$) and lower ($z < 0$) parts of the domain are indicated by the solid and dashed lines, respectively. The corresponding evolution of the total density $\rho(t, x, z)$ defined by Eq. 21

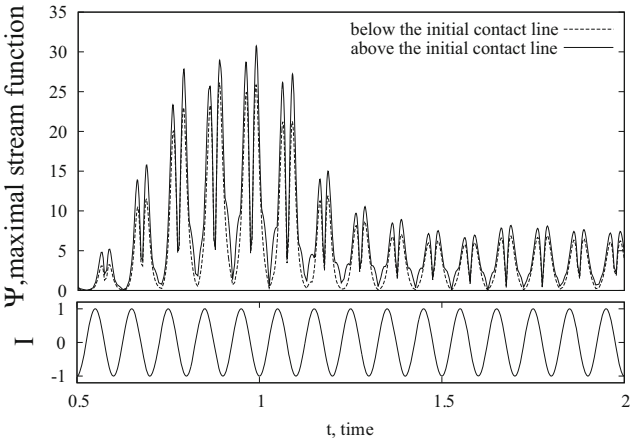

Fig. 6 Time evolution of the maximal stream function (*top*) under the influence of a periodically varying inertial field $I(t)$ (*bottom*) with the amplitude $\mu = 4$ and period $\tau = 0.1$. The values calculated for the *lower* and *upper* layer are indicated by the *dashed* and *solid line*, respectively

is illustrated by the frames for three consecutive moments of time in Fig. 5 during one period of vibrations. Taking into account that the time has been put in the dimensionless form by using the characteristic diffusive time, the oscillation of the inertial field with the period $\tau = 0.1$ should be considered as low-frequency vibrations.

We found that the pure reaction-diffusion process similar to those in the static case also takes place when the system is under the influence of vibrations. But this stage lasts not for long: after $t > 0.3$ one can observe the exponential growth of the critical disturbances. We found that the vibrations parametrically excite the synchronous response of the system (Fig. 6). It can be noted that this excitation of the convective instability occurs almost simultaneously both at the bottom and top of the domain. The stream function reaches its maximum at about $t \approx 1$ and then slightly decreases tending to some quasi-equilibrium value.

The time series of the stream function shown in Fig. 6 has two characteristic peaks within one period of vibration. The origin of these peaks becomes clear from Fig. 3. When the direction of the inertial field reverses sign, the zones of unstable density stratification right of both minima (Fig. 3, top) are replaced by the unstable stratification zones adjacent to the minima on the left (Fig. 3, bottom). Thus, during the first half cycle of vibration the most dangerous perturbations are the DLC and CDD instabilities having double-diffusive nature (Fig. 7, top frames, $t = \tau/3$). During the second half cycle the DLC and CDD instabilities begin to decay, and the most dangerous perturbations are excited via the Rayleigh-Taylor mechanism of the instability (Fig. 7, bottom frames, $t = \tau$). The intermediate frames shown in Fig. 7 at $t = 2\tau/3$ represent the mixed-mode convection, when all kinds of instabilities are active and coexist simultaneously in real-time. Technically, it looks like the oscillations of the spatial location of the convective vortices near the local maximum density. Consequently, the vibrations help to merge two regions (separated in the static case) into a single entity with the joint mass transfer.

Thus, the combined effect of the processes of reaction-diffusion and vibrations of low frequency applied in the perpendicular direction to the reaction front may result in the development of the localized cellular convection within the bulk of almost motionless liquid.

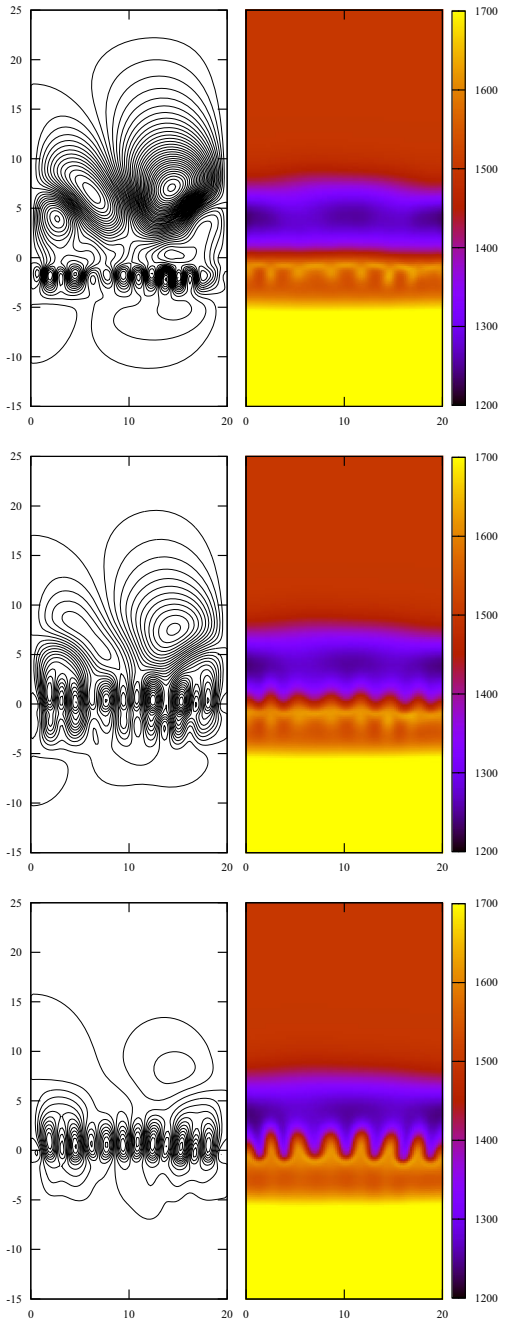

Fig. 7 Temporal evolution of the stream function $\Psi(t, x, z)$ (*left*) and total density $\rho(t, x, z)$ (*right*). The frames from *up* to *down* pertain to times $t = \tau/3, 2\tau/3, \tau$ during one vibrations period τ, respectively. The domain of integration is $0 < x < 40$, $-30 < z < 30$, but only part of the full domain is shown: $0 < x < 20$, $-15 < z < 25$. The *line* $z = 0$ corresponds to the initial contact line between layers

Experimental Observations

Let us discuss the results of experiments obtained under the condition of the static gravity. The experiments were performed in a vertically oriented Hele-Shaw cell made of two glass plates (width 2.5 cm × height 9.0 cm) separated by a thin gap of 0.12 cm. The cell was filled with aqueous solutions of nitric acid HNO_3 (the upper layer) and sodium hydroxide NaOH (the bottom layer) whose concentration always provided a steady stratified density distribution. During the filling of the cell with the upper solution, the lower layer was separated by a thin plastic slide inserted in two narrow (0.3 mm) slots made in the walls (the initial contact line can be seen in Fig. 8). In order to visualize a

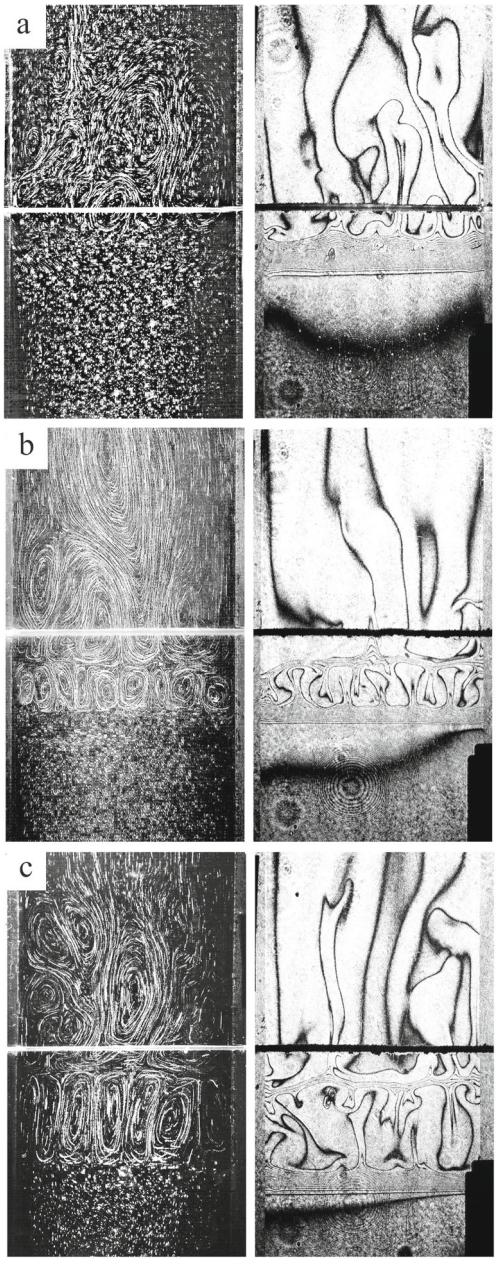

Fig. 8 Velocity field (*left*) and interferogram (*right*) obtained at different time moments after the start of the experiment with aqueous solutions of nitric acid HNO_3 above and sodium hydroxide NaOH below: **a** - 300 s; **b** - 1100 s; **c** - 2250 s. Initial concentrations of acid and base are the same and equal 1 mol/l

refractive index distribution, we have used Fizeau interferometry. The distribution of the refractive index is caused by inhomogeneities induced by the concentration distribution of species and reaction exothermicity. The latter was found to be negligible because the deviation due to temperature was at least one order of magnitude smaller than that caused by concentration. Silver-coated hollow glass spheres were added to the liquids to observe the convective patterns which form during the reaction.

The Fig. 8 demonstrates the evolution of the velocity (left) and concentration (right) during formation of the cellular convective structure under the static gravity. Right after the prepared solutions were brought into contact, the transition zone started to form between them where the reagents were transported towards the reaction front only via the diffusion mechanism. Then the occurrence of a depleted layer just above the diffusion zone has given rise to the formation of plumes clearly visible in Fig. 8a which result in the development of weak buoyancy-driven convection in the whole upper layer (the DLC instability).

One can see that before the cells appear there forms a depression of the interference fringes above the reaction front (see Fig. 8a, right). It indicates the occurrence of inflection on the density profile and therefore the formation of the "density pocket". Thus, a few minutes after the beginning of the experiment, the fluid flow in the form of the periodic array of convective cells (Fig. 8b) has been formed within the diffusion zone just above the reaction front. The cells of which have appeared due to the CDD instability were arranged between two areas of immobile fluid which definitely indicated the formation of a local "pocket" with the unstable density stratification. One can note that the cellular structure did not interact directly with the DLC convection in the upper layer (Fig. 8b,c).

We have found that the structure can exist for several hours with the band slowly widening with time that results in the wavelength growth (Fig. 9). As in the experiment, the boundaries of the structure obtained numerically slowly move apart with time (Fig. 5). For example, at $t = 3$ the pattern wavelength is about 4.2 (in dimensionless units), which is in good agreement with the experimental data (Fig. 9).

Thus, the experimental observations presented in Figs. 8 and 9 reveal a good agreement with the results of the numerical simulations for the development of the CDD convection.

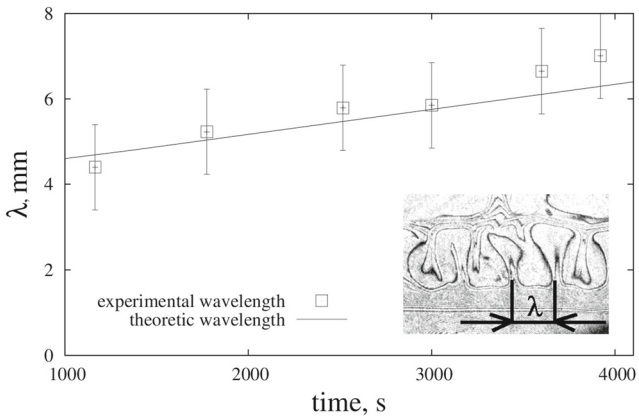

Fig. 9 Time evolution of the wavelength of the CDD pattern in time obtained experimentally (*squares*) and numerically within the theoretical model (*solid line*)

Conclusions

We have considered the development of the convective instability in a two-layer system of miscible liquids placed in a narrow vertical gap of the Hele-Shaw cell. The upper and lower layers are formed, respectively, with aqueous solutions of acid and base with the strong concentration-dependence of the diffusion coefficients. When the layers are brought into contact, the frontal neutralization reaction $A + B \rightarrow S$ starts. Since this system was found to be sensitive to the inertia, we have studied the influence of the static and periodic inertial field. The mathematical model has been developed on the base of a system of reaction-diffusion-convection equations written within a Hele-Shaw approximation. The laws of diffusion coefficients for species have been evaluated on the base of the data for a specific pair of reagents: the nitric acid HNO_3 and sodium hydroxide NaOH. In the static gravity, we have found that two kinds of instabilities develop in the vicinity of the reaction front: one of them is the diffusive layer convection occurring traditionally in such problems, and a new type, the concentration-dependent diffusion instability that arises when the diffusion coefficients of species depend on their concentrations. The important feature of the latter chemo-convective pattern is its localization within the reaction zone and the periodicity of convective cells along the reaction front. In the case of the periodically varied inertia, we have found the mixed-mode instability which represents a combination of the instabilities of double-diffusive nature (the DLC and CDD instabilities) and the Rayleigh-Taylor mechanism of the convection. The experimental part of the study was carried out for the case of the static gravity. Flow visualization was made using interferometry and adding the light-scattering particles to the flow. The obtained results of the numerical simulations was found to be in good agreement with the experimental observations.

Acknowledgments The work was supported by the Russian Fund for Basic Research (project 16-31-00251_mol_a) and Ministry of Education of Perm Region (grant C-26/004.04).

References

Aitova, E.V., Bratsun, D.A., Kostarev, K.G., Mizev, A.I., Mosheva, E.A.: Effect of concentration-dependent diffusion on pattern formation in two-layer system of reacting miscible liquids. Comput Continuum Mech **8**(4), 345–358 (2015)

Allali, K., Volpert, V., Pojman, J.A.: Influence of vibrations on convective instability of polymerization fronts. J. Eng. Math. **41**(1), 13–31 (2002)

Almarcha, C., Trevelyan, P.M.J., Grosfils, P., De Wit, A.: Chemically driven hydrodynamic instabilities. Phys. Rev. Lett. **104**(4), 044501 (2010)

Almarcha, C., R'Honi, Y., De Decker, Y., Trevelyan, P.M.J., Eckert, K., De Wit, A.: Convective mixing induced by acid-base reactions. J. Phys. Chem. **115**(32), 9739–9744 (2011)

Bratsun, D.A.: Effect of unsteady forces on the stability of non-isothermal particulate flow under finite-frequency vibrations. Microgravity Sci. Technol. **21**(Suppl. 1), 153–158 (2009)

Bratsun, D.A.: On Rayleigh-Bénard mechanism of alignment of salt fingers in reactive immiscible two-layer systems. Microgravity Sci. Technol. **26**, 12–35 (2014)

Bratsun, D.A., De Wit, A.: On Marangoni convective patterns driven by an exothermic chemical reaction in two-layer systems. Phys. Fluids **16**, 1082–1096 (2004)

Bratsun, D.A., De Wit, A.: Buoyancy-driven pattern formation in reactive immiscible two-layer systems. Chem. Eng. Sci. **66**(22), 5723–5734 (2011)

Bratsun, D.A., Teplov, V.S.: On the stability of the pulsed convective flow with small heavy particles. Eur. Phys. J. A. P. **10**, 219–230 (2000)

Bratsun, D., Kostarev, K., Mizev, A., Mosheva, E.: Concentration-dependent diffusion instability in reactive miscible fluids. Phys. Rev. E **92**, 011003 (2015)

Carballido-Landeira, J., Trevelyan, P.M.J., Almarcha, C., De Wit, A.: Mixed-mode instability of a miscible interface due to coupling between Rayleigh-Taylor and double-diffusive convective modes. Phys. Fluids **25**(2), 024107 (2013)

Crank, J.: The Mathematics of Diffusion. Clarendon Press, Oxford (1975)

Eckert, K., Rongy, L., De Wit, A.: $A + B \rightarrow C$ reaction fronts in Hele-Shaw cells under modulated gravitational acceleration. Phys. Chem. Chem. Phys. **14**, 7337–7345 (2012)

Fernandez, J., Kurowski, P., Petitjeans, P., Meiburg, E.: Density-driven unstable flows of miscible fluids in a Hele-Shaw cell. J. Fluid Mech. **451**, 239–260 (2002)

Gaponenko, Y.A., Torregrosa, M., Yasnou, V., Mialdun, A., Shevtsova, V.: Dynamics of the interface between miscible liquids subjected to horizontal vibration. J. Fluid Mech. **784**, 342–372 (2015)

Gershuni, G.Z., Zukhovitskii, E.M.: Parametric excitation of convective instability. J. Appl. Math. Mech. **27**, 1197–1203 (1963)

Hickernell, F.J., Yortsos, Y.C.: Linear stability of miscible displacement processes in porous media in the absence of dispersion. Stud. Appl. Math. **74**, 93–115 (1986)

Homsy, G.M.: Viscous fingering in porous media. Ann. Rev. Fluid Mech. **19**, 271–311 (1987)

Lemaigre, L., Budroni, M.A., Riolfo, L.A., Grosfils, P., De Wit, A.: Asymmetric Rayleigh-Taylor double-diffusive fingers in reactive systems. Phys. Fluids **25**, 385–399 (2013)

Loggia, D., Rakotomalala, N., Salin, D., Yortsos, Y.C.: Evidence of new instability thresholds in miscible displacements in porous media. Europhys. Lett. **32**, 633–638 (1995)

Manickam, O., Homsy, G.M.: Stability of miscible displacements in porous media with nonmonotonic viscosity profiles. Phys. Fluids **5**, 1356–1367 (1993)

Manickam, O., Homsy, G.M.: Simulation of viscous fingering in miscible displacements with nonmonotonic viscosity profiles. Phys. Fluids **6**, 95–107 (1994)

Manickam, O., Homsy, G.M.: Fingering instabilities in vertical miscible displacement flows in porous media. J. Fluid Mech. **288**, 75–102 (1995)

Martin, J., Rakotomalala, N., Salin, D.: Gravitational instability of miscible fluids in a Hele-Shaw cell. Phys. Fluids **14**, 902–905 (2002a)

Martin, J., Rakotomalala, N., Salin, D., Bockmann, M.: Buoyancy-driven instability of an autocatalytic reaction front in a Hele-Shaw cell. Phys. Rev. E **65**, 051605 (2002b)

Martin, J., Rakotomalala, N., Talon, L., Salin, D.: Viscous lock-exchange in rectangular channels. J. Fluid Mech. **673**, 132–146 (2011)

Putin, G.F., Zavarykin, M.P., Zorin, S.V., Zyuzgin, A.V.: Heat and mass trans-fer in the variable inertia field. In: Proceeding of the 8th European symposium on materials and fluid sciences in microgravity, pp. 99–102. ESA Publ. Division, Brussels (1992)

Rogers, J.L., Schatz, M.F., Bougie, J.L., Swift, J.B.: Rayleigh-Bénard convection in a vertically oscillated fluid layer. Phys. Rev. Lett. **84**(1), 87–90 (2000)

Ruyer-Quil, Ch.: Inertial corrections to the Darcy law in a Hele-Shaw cell. C. R. Acad. Sci. Paris **329**(Série IIb), 1–6 (2001)

Trevelyan, P.M.J., Almarcha, C., De Wit, A.: Buoyancy-driven instabilities around miscible $A + B \rightarrow C$ reaction fronts: A general classification. Phys. Rev. E **91**(2), 023001 (2015)

Turner, J.S.: Double-diffusive phenomena. Ann. Rev. Fluid Mech. **6**, 37–54 (1974)

von Kameke, A., Huhn, F., Fernandez-Garcia, G., Munuzuri, A.P., Perez-Munuzuri, V.: Propagation of a chemical wave front in a quasi-two-dimensional superdiffusive flow. Phys. Rev. E **81**, 066211 (2010)

von Kameke, A., Huhn, F., Munuzuri, A.P., Perez-Munuzuri, V.: Measurement of large spiral and target waves in chemical reaction-diffusion-advection systems: Turbulent diffusion enhances pattern formation. Phys. Rev. Lett. **110**, 088302 (2013)

Zeng, J., Yortsos, Y.C., Salin, D.: On the Brinkman correction in unidirectional Hele-Shaw flows. Phys. Fluids **15**, 3829–3836 (2003)